



Efficiency enhancement in dye-sensitized solar cells with down conversion material ZnO: Eu³⁺, Dy³⁺



Nannan Yao^a, Jinzhao Huang^{a,*}, Ke Fu^a, Shiyong Liu^a, Dong E^a, Yanhao Wang^a, Xijin Xu^{a,*}, Min Zhu^b, Bingqiang Cao^{b,*}

^a School of Physics and Technology, University of Jinan, Jinan 250022, Shandong Province, PR China

^b Key Laboratory of Inorganic Functional Materials in Universities of Shandong, School of Materials Science and Engineering, University of Jinan, Jinan 250022, Shandong Province, PR China

HIGHLIGHTS

- The ZnO: Eu³⁺, Dy³⁺ can broaden absorption region of solar spectrum in DSSCs.
- The enhanced carrier transportation is achieved.
- The TiO₂/G/ZnO: Eu³⁺, Dy³⁺ can improve the efficiency of DSSCs dramatically.
- A possible mechanism for the TiO₂/G/ZnO: Eu³⁺, Dy³⁺ structure is proposed.

ARTICLE INFO

Article history:

Received 8 February 2014

Received in revised form

22 May 2014

Accepted 23 May 2014

Available online 4 June 2014

Keywords:

Dye-sensitized solar cells

Down conversion

ZnO: Eu³⁺, Dy³⁺

Graphene

ABSTRACT

The down conversion (DC) material ZnO: Eu³⁺, Dy³⁺ are synthesized by precipitation method and used to prepare the photo anode of dye-sensitized solar cells (DSSCs). The effects of down conversion material on the photoelectric performance of the DSSC were characterized by the X-ray diffraction (XRD), photoluminescence (PL), scanning electron microscope (SEM), current–voltage (*I*–*V*) curve, incident-photon-to-current conversion efficiency (IPCE) and UV–vis–NIR absorption spectroscopy. In this paper, Eu³⁺, Dy³⁺ codoped ZnO excited by from UV to blue light converts blue to red light emission, corresponding to the absorption region of the dye (N719). At the concentration 1.75% of ZnO: Eu³⁺, Dy³⁺ (weight ratio of DC to TiO₂), the short-circuit current density and conversion efficiency of the DSSCs reached to the optimal values: 8.92 mA cm^{−2} and 4.48%, about 212% and 245% higher than with pure TiO₂ and about 91.4% and 105% higher than with TiO₂/graphene (G) structure, respectively. The research result reveals that the application of DC material can improve the efficiency of DSSCs.

© 2014 Elsevier B.V. All rights reserved.

1. Introduction

Dye-sensitized solar cells (DSSCs) have attracted much attention as a renewable energy source due to their high performance, low cost, easy fabrication procedures, and so on [1–3]. Typically, DSSCs consist of a TiO₂ semiconductor electrode, Ru complex dye, an iodine-based electrolyte and Pt counter electrode [4]. Presently, the power conversion efficiency of the DSSCs has been already exceeded 12% [5]. One problem that confines the efficiency enhancement is that photo anode has a maximum absorption in the visible region

of the total incident solar irradiation, in other words, approximately 50% of solar irradiation energy in the ultraviolet and infrared regions is not utilized [6,7]. To extend light absorption and improve the conversion efficiency, lots of research efforts have been focused on modifying the anode of DSSCs for matching the spectral response to the solar spectrum [8,9]. Recently, Q. Wang and co-workers have achieved a high efficiency of 10.8% by adding small quantities of Au nanoparticles into TiO₂ photoanodes [10]. This success provides a very useful approach to achieve efficient light harvesting and charge separation in DSSCs. Moreover, using rare earth (RE) ions is another good choice to extend light absorption [11]. As we all know that RE elements luminescence covers a wide range, from the near-infrared, through the visible to the ultraviolet [12]. The utilization of a luminescence layer composed of up-conversion (UC) or down conversion (DC) materials has been

* Corresponding authors.

E-mail addresses: ss_huangjinzhao@ujn.edu.cn, jzhuangjz@hotmail.com (J. Huang).

widely reported. The UC effects have been used previously to enhance the device efficiencies of DSSCs. For example, G. P. Demopoulos et al., in 2010 reported on UC application in DSSCs [13]. They inserted Yb/Er UC particles into the amorphous TiO₂ scattering layer to help capture near-infrared (NIR) light by converting it into visible light absorbable by the dye and realized higher conversion efficiency and photocurrent output. The application of DC material in DSSCs was reported by T. S. Atabaev and coworkers [14]. They fabricated an FTO/TiO₂/phosphor multilayered photoelectrode by depositing SrAl₂O₄:Eu²⁺, Dy³⁺ on a porous TiO₂ film. The SrAl₂O₄:Eu²⁺, Dy³⁺ particles shift the shorted UV wavelengths into the main absorption range of the dye and an efficiency of 6.85% was obtained. Our work in this paper is focusing on DC effects in DSSCs.

Lanthanide-based NPs have attracted significant attention for its harvest ability of the UV-blue part of solar spectrum [15–17]. DC materials have been investigated for decades to enhance performance of solar cells and were first reported by T. Trupke et al. [18]. In our work, we use ZnO as matrix material due to its stable chemical properties, high electron mobility, easy fabrication procedures, and by doping rare earth in ZnO can realize a high photoluminescence of rare earth ion [19]. To our knowledge, the usage of TiO₂/G/ZnO: Eu³⁺, Dy³⁺ structure in DSSCs has not yet been reported in the literature.

In this paper, a multifunctional TiO₂/G/ZnO: Eu³⁺, Dy³⁺ composite films are for the first time applied to construct photo anode of DSSCs. Eu³⁺, Dy³⁺ codoped ZnO has a wide UV to blue light absorption and converts it into visible light that matches the absorption region of the commonly used dye N719. In addition, graphene is an interesting two-dimensional carbon allotrope that has attracted considerable research interest because of its unique structure and superior properties such as high carrier mobility. Here, the graphene loading can not only reduce the electrolyte–electrode interfacial resistance and the charge recombination rate, but also enhance the transport of electrons from the films to the fluorine doped tin oxide (FTO) substrates [20–22]. By incorporating 1.75 wt % ZnO: Eu³⁺, Dy³⁺ and 0.5 wt% graphene in the TiO₂ photo anode, the short-circuit current density and conversion efficiency of the DSSCs are as high as 8.92 mA cm⁻² and 4.48%.

2. Experimental

2.1. Synthesis of ZnO: Eu³⁺, Dy³⁺

4.435 g Zn(OOCCH₃)₂·2H₂O was dissolved in the mixture solution (37.5 ml ethanol and 25 ml deionization water). 0.0705 g europium oxide was dissolved in nitric acid. The two solutions were mixed to form the mole ratio of Zn²⁺ to Eu³⁺ (or Dy³⁺) 1:0.02, and the mole ratio of Eu³⁺ to Dy³⁺ is 1:1. Then the solution was stirred for 20 min under 30 °C, and the solution became transparent liquid. The sodium acetate was gradually added to the above solution until pH of the solution is about 6, then the 0.5 ml acetoxyacetone was added to act as surface active agent. With the addition of 1.715 g sodium hydroxide, the solution turned into a white suspension. The white precipitation was obtained by filtering and drying in oven at 90 °C. Finally, the ZnO: Eu³⁺, Dy³⁺ powder was calcined in furnace at 150 °C for 1 h.

2.2. Fabrication of DSSCs

Firstly, 1 g of P25 was dispersed in a mixed solution of distilled water (2.5 ml), acetylacetone (35 μl) and two drops of Triton X-100. In order to suppress the recombination of electron and hole, adding 0.3 ml MgO solution in the TiO₂ pastes. Briefly, 0.0026 g of MgO was dissolved into a solution consisting of 1 ml distilled water and

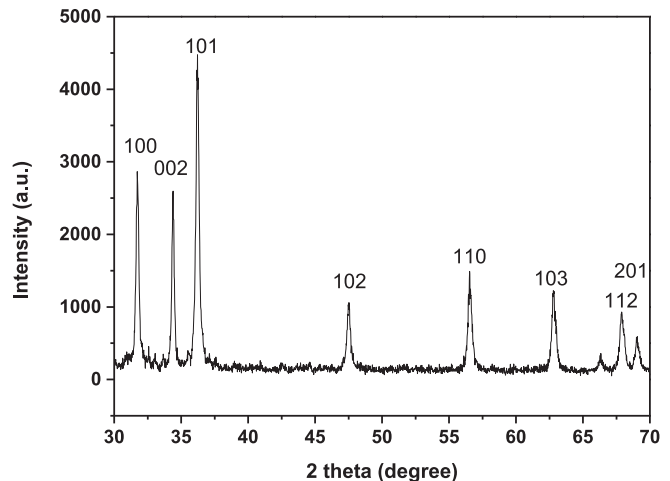


Fig. 1. XRD pattern of ZnO: Eu³⁺, Dy³⁺.

1.5 ml acetic acid (with a concentration of 36 wt %). To prepare the TiO₂/G/ZnO: Eu³⁺, Dy³⁺ composite film electrodes, 5 mg graphene and a varying amount of ZnO: Eu³⁺, Dy³⁺ were added in the pastes under vigorous stirring for 24 h at room temperature. To confirm the effect of the down conversion material, the weight percentages of ZnO: Eu³⁺, Dy³⁺ in the composite films were 0, 0.5, 1.5, 1.75, 2.0, 2.25, and 2.5 wt%.

Prior to the fabrication of DSSCs, FTO glass substrates were first cleaned with detergent and ethanol, respectively, and ultrasonicated in acetone, ethanol and deionized water for 20 min in turn, then rinsed with a large amount of distilled water and lastly dried at 80 °C. The TiO₂/G/ZnO: Eu³⁺, Dy³⁺ electrodes were prepared on FTO coated glass substrates by the doctor blade method [23]. The TiO₂/G/ZnO: Eu³⁺, Dy³⁺ composite films were further heated to 450 °C for 30 min. After cooling to room temperature, the films were treated with an aqueous solution of TiCl₄ (7.5 mg ml⁻¹) at 70 °C for 30 min, and then rinsed with deionized water and ethanol in sequence. Finally, the films were sintered at 450 °C for 30 min. After cooling down to 80 °C, the electrodes were immersed into a 0.36 mM N719 ruthenium dye ethanol solution for 24 h at room temperature and finally rinsed with ethanol to remove the nonchemisorbed dye. Pt counter electrode was prepared by spin-coating onto the FTO surface at 1000 rpm for 20 s for three times, followed by annealing at 450 °C for 30 min. Subsequently, fix the sensitized photoelectrode and counter electrode together using a hot-melt film spacer. Finally, a dye-sensitized solar cell was assembled by injecting electrolyte (OPV-MPN-I) into the space between the electrodes.

2.3. Material and cell characterization

The structure of the ZnO: Eu³⁺, Dy³⁺ was investigated by XRD using a D8 ADVANCE with Cu K_α at λ = 0.15406 nm. The PL was measured using the FLS920 fluorescent spectrometer made by Edinburgh Instruments using a Xe lamp as the excitation source. The absorption spectra of N719 dye was examined with a UV–vis–NIR spectrophotometer (TU-1901). The morphology of anode films were examined with field emission scanning electron microscope (FE-SEM, Quanta FEG250). The I–V characteristics of the DSSCs were measured with a Keithley 2612A source/meter under simulated sunlight (AM1.5, 100 mWcm⁻², San-Ei). The IPCE was measured with a QEX10 system (PV Measurement Inc.). The irradiation areas of the working electrode were about 0.16 cm². All of these measurements were carried out at room temperature.

3. Results and discussion

The XRD is used to characterize the crystal structures of ZnO: Eu³⁺, Dy³⁺. The XRD pattern of ZnO: Eu³⁺, Dy³⁺ is shown in Fig. 1. The observed main diffraction peaks can be indexed to ZnO with hexagonal wurtzite structure (JCPDS No. 36-1451). The diffraction peaks related to Eu₂O₃ and Dy₂O₃ cannot be observable. It indicates that the Eu³⁺ and Dy³⁺ have been incorporated into the lattice of ZnO. In the Fig. 1, the sharp diffraction peaks can confirm that the samples are well crystallized, and it is favorable to be used in the photo anode of DSSCs.

The solar radiation spectrum, absorption spectrum, photoluminescence excitation (PLE) and PL of ZnO: Eu³⁺, Dy³⁺ are shown in the Fig. 2. The excitation spectrum of ZnO: Eu³⁺, Dy³⁺ (Fig. 2(c)) shows a strong absorption peak near 338 nm and 394 nm, which are about near the maximum of solar radiation. The emission spectrum of ZnO: Eu³⁺, Dy³⁺ are presented in Fig. 2(d). The emission 483 nm and 575 nm of Dy³⁺ corresponding to ⁴F_{9/2}–⁶H_{15/2} and ⁴F_{9/2}–⁶H_{13/2} transition of the Dy³⁺ respectively are observed. Besides, the emission 394 nm, 458 nm, 593 nm and 611 nm which is from the transition from ⁵L₆–⁷F₀, ⁵D₂–⁷F₀, ⁵D₀–⁷F₂ and ⁵D₀–⁷F₁ of Eu³⁺ are obtained. The emission spectrum of Eu³⁺ and Dy³⁺ almost locate in the visible region and match well with the absorption region of the dye. The most conventionally used Ru dyes (e.g., N719, N749) with a band-gap of 1.8 eV responds well only in the visible range [24]. The absorption spectra of N719 dye examined by UV–visible spectroscopy is shown in Fig. 2(b). We can see from the graph, there is strong absorption in visible light, especially a strong absorption peak at 532 nm, which can better overlap with the PL of ZnO: Eu³⁺, Dy³⁺. Therefore, with the addition of ZnO: Eu³⁺, Dy³⁺

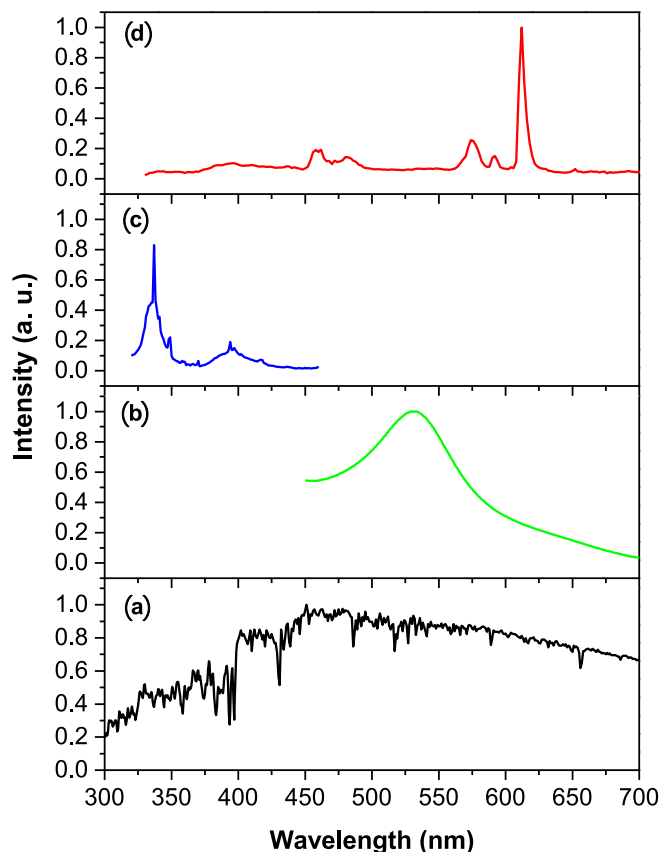


Fig. 2. (a) Spectrum of solar radiation; (b) Absorption of N719; (c) PLE of ZnO: Eu³⁺, Dy³⁺; (d) PL of ZnO: Eu³⁺, Dy³⁺.

into TiO₂ paste as the photo anode, the absorption spectrum of N719 can be extended. Consequently, the performances maybe improved effectively in DSSCs. In order to verify the function of ZnO: Eu³⁺, Dy³⁺, the absorption spectrum of the pure TiO₂ and TiO₂/G/ZnO: Eu³⁺, Dy³⁺ composite film are measured. The result is shown in the Fig. 3. It can be seen the absorption intensity is enhanced after the incorporation of ZnO: Eu³⁺, Dy³⁺.

Fig. 4 shows the cross-section and surface SEM images of different anode with pure TiO₂ film and TiO₂/G/ZnO: Eu³⁺, Dy³⁺ composite film. The thickness of pure TiO₂ film shown in Fig. 4(a) is nearly same with the TiO₂/G/ZnO: Eu³⁺, Dy³⁺ composite film shown in Fig. 4(c). Moreover, the surface morphology of the different anode with pure TiO₂ film and TiO₂/G/ZnO: Eu³⁺, Dy³⁺ composite film is nearly same (shown in Fig. 4(b) and (d) respectively). So the effect of the porosity of the films on the efficiency is small in our work, and the doped ZnO with rare earth is a dominant factor to affect the property of the solar cells.

In order to verify the effect of the porosity of the films on the quantity of the dye in the films is small further, that is to say, the different photoanodes have the same dye absorption quantity. The dye desorption from photoanodes method is applied [25]. 0.024 g NaOH was dissolved into a mix solution of 3 ml distilled water and 3 ml ethanol, and then the different photoanodes sensitized by dye were immersed in NaOH solution for 5 min respectively, so that the N719 desorbed from the photo anode can be completely dissolved into the solution. After desorption, the absorption spectrum of pure TiO₂ film and TiO₂/G/ZnO: Eu³⁺, Dy³⁺ composite film were determined and the result is shown in Fig. 5 (a). The absorption peak of N719 is not observed, showing that dye molecules are completely dissolved into the solution. In addition, the absorption spectra of N719 desorbed from the different photoanodes were measured. The result in Fig. 5 (b) shows that the absorption of dye desorbed from pure TiO₂ film and TiO₂/G/ZnO: Eu³⁺, Dy³⁺ composite film is nearly same. From Fig. 5(a) and (b), we can see that the absorption of TiO₂/G/ZnO: Eu³⁺, Dy³⁺ composite film is higher than pure TiO₂ film after desorption, and the absorption of dye desorbed from pure TiO₂ film is higher than TiO₂/G/ZnO: Eu³⁺, Dy³⁺ composite film, indicating the absorbance of N719 dye is nearly same in each sample.

Fig. 6 shows the photovoltaic performances of the DSSCs based on different photoanodes. The corresponding photovoltaic parameters are summarized in Table 1. The typical DSSC using pure TiO₂ as photo anode possesses an efficiency of 1.30% and a fill factor (FF) of

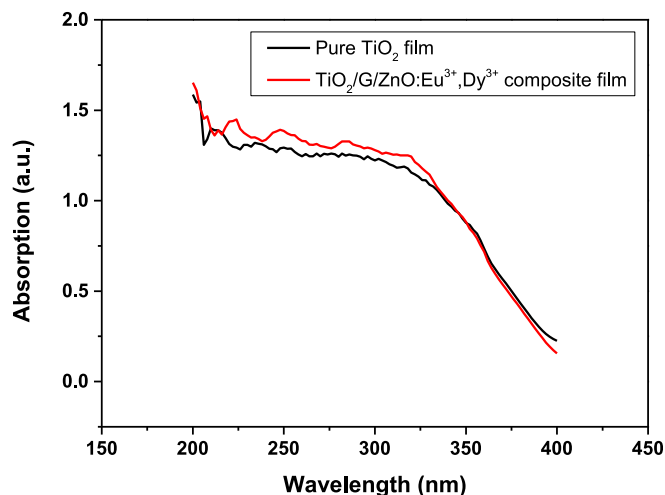


Fig. 3. The absorption spectrum of pure TiO₂ and TiO₂/G/ZnO: Eu³⁺, Dy³⁺ composite film.

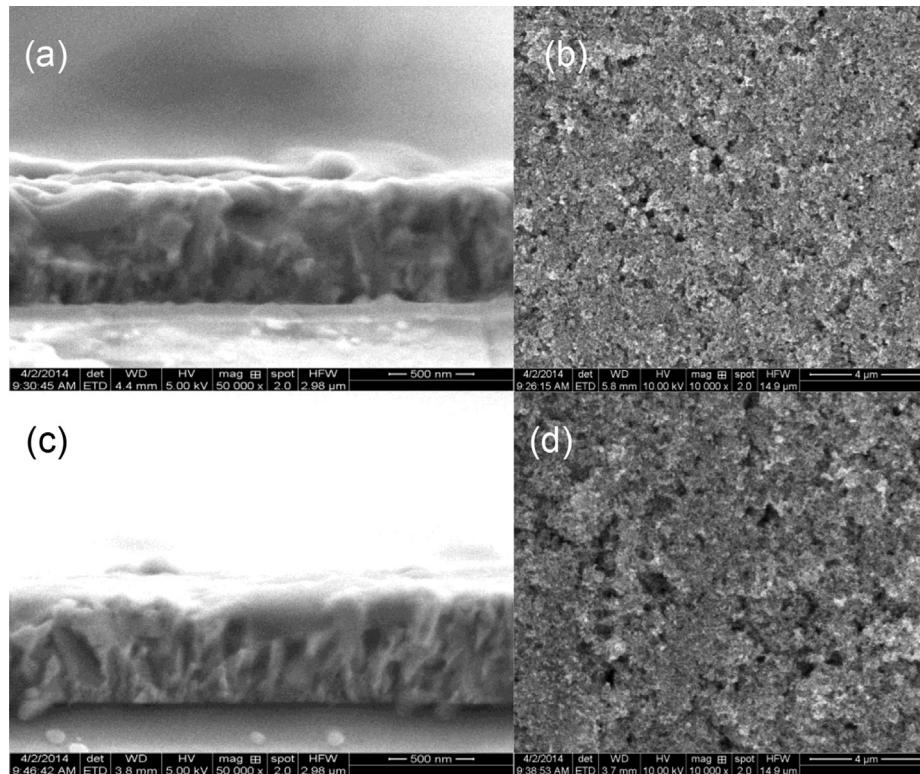


Fig. 4. SEM images of FTO/TiO₂ cross-section (a), and top view (b), SEM images of FTO/TiO₂/G/ZnO: Eu³⁺, Dy³⁺ cross-section (c), and top view (d).

0.63. The parameters show that the device performance is dramatically improved through the insertion of graphene. After doping 0.5 wt % graphene into TiO₂, the short-circuit current density of 4.66 mA cm⁻² is achieved, while the efficiency increases from 1.30% to 2.19%. This suggests that graphene acted as a charge-carrier pathway, reducing the charge recombination rate and enhancing the transport of electrons [18].

In addition, with the insertion of DC material, the performance of solar cells is also highly improved. ZnO: Eu³⁺, Dy³⁺ can absorb UV to blue photons in the solar spectrum and convert them into the visible emission, extending the absorption region of the dye (N719), which has been confirmed from the above PL measurements. Here, we doped ZnO: Eu³⁺, Dy³⁺ with different concentrations into the TiO₂ pastes to optimize the cell performance. By incorporating 1.75 wt% ZnO: Eu³⁺, Dy³⁺ and 0.5 wt% graphene in the TiO₂ photo anode, an optimal result was achieved with an efficiency of 4.48%.

The IPCE is an important parameter of the solar cell which directly measures how efficiently the incident photons are converted to electrons [26]. As shown in Fig. 7, a high value observed near 350 nm can be ascribed to the absorption of TiO₂ [27]. Furthermore, the IPCE of the DSSCs based on TiO₂/G/ZnO: Eu³⁺, Dy³⁺ structure was higher in both the UV and visible regions than pure TiO₂ structure. It is observed that the solar cell with the 1.75 wt % DC doping concentration shows the highest IPCE, which is in agreement with the *I*–*V* result. With the insertion of ZnO: Eu³⁺, Dy³⁺, an apparent increase in IPCE in the range from 500 to 550 nm could be observed. The ZnO: Eu³⁺, Dy³⁺ could absorb the UV to blue part of solar radiation and then convert them into the visible light which matches the strong absorbing region of the dye. Consequently, the efficiency is increased. So, doping DC materials is beneficial to increase the IPCE in DSSCs.

A possible mechanism for the TiO₂/G/ZnO: Eu³⁺, Dy³⁺ structure is proposed, as illustrated in Fig. 8. Upon the light irradiation, the

ZnO: Eu³⁺, Dy³⁺ convert UV to blue of solar irradiation into visible light, which can extend the absorption range of N719. After the dye molecules are excited, they will give up the electron and inject it into the adjacent TiO₂. The injected electrons will reach the FTO glass of the anode through the TiO₂. Moreover, the graphene can provide another way to transport the electron. The role of the graphene is not only enhancing the transport of electrons from the composite films to the FTO, but reducing the electrolyte–electrode interfacial resistance and the charge recombination rate. Finally the electrons move to the Pt counter electrode via the external circuit, and the redox couple in the electrolyte can transport electrons from the counter electrode to the oxidized dye molecules.

4. Conclusions

In summary, the DC material ZnO: Eu³⁺, Dy³⁺ was synthesized and introduced into the DSSCs. A multifunctional TiO₂/G/ZnO: Eu³⁺, Dy³⁺ composite films were applied to construct photo anode of DSSCs. This novel structure showed an excellent capacity to extend light absorption by converting UV to blue part of solar radiation to visible light that corresponds to the main absorption region of N719. With addition of 0.5 wt % graphene into TiO₂, the short-circuit current density increased from 2.86 mA cm⁻² to 4.66 mA cm⁻², it demonstrated that graphene reduced the charge recombination rate and enhanced the transport of electrons. By incorporating 1.75 wt % ZnO: Eu³⁺, Dy³⁺ and 0.5 wt % graphene in the TiO₂, a short-circuit current density of 8.92 mA cm⁻² was achieved and the conversion efficiency reached as high as 4.48%. In addition, the 1.75 wt % DC doping concentration shows the highest IPCE, which is in agreement with the results of *I*–*V* curve. The research results reveal that the DC material ZnO: Eu³⁺, Dy³⁺ is helpful to improve the performance of DSSCs.

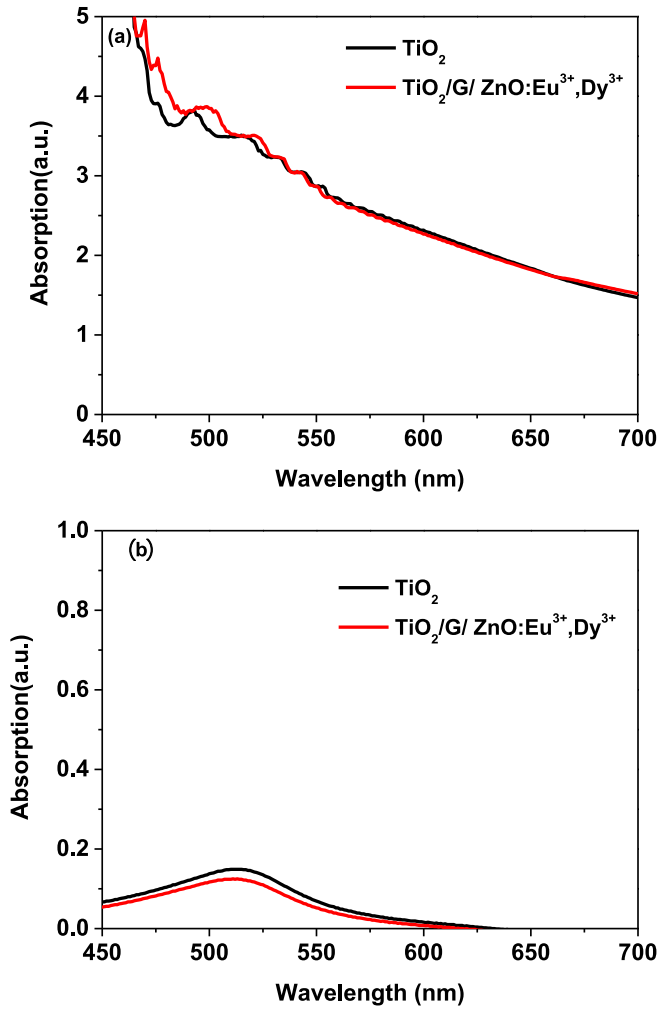


Fig. 5. (a) The absorption spectrum of pure TiO₂ film and TiO₂/G/ZnO: Eu³⁺, Dy³⁺ composite film after desorption; (b) The absorption spectra of N719 desorbed from pure TiO₂ film and TiO₂/G/ZnO: Eu³⁺, Dy³⁺ composite film.

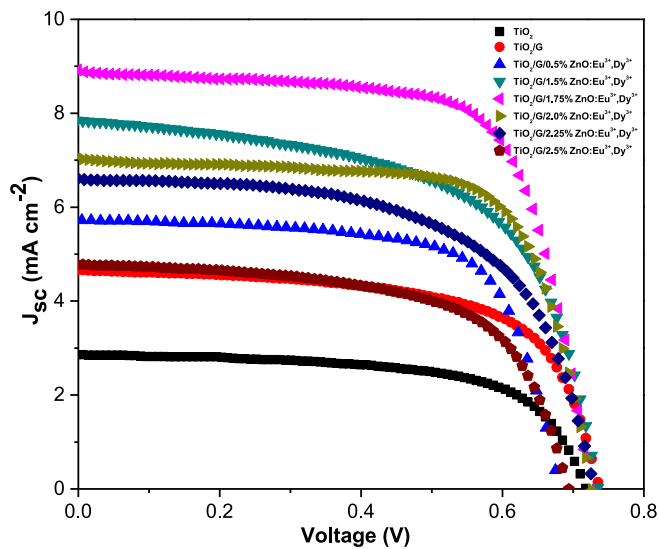


Fig. 6. Photocurrent-voltage curves of DSSCs based on different photoanodes.

Table 1

Photovoltaic parameters (short-circuit current density, open-circuit voltage, fill factor, and efficiency) of the DSSCs using different photoelectrode structures.

Photo anode	J _{sc} (mA cm ⁻²)	V _{oc} (V)	FF	η(%)
TiO ₂	2.86	0.72	0.63	1.30
TiO ₂ /G	4.66	0.74	0.64	2.19
TiO ₂ /G/0.5%ZnO: Eu ³⁺ , Dy ³⁺	5.72	0.68	0.69	2.67
TiO ₂ /G/1.5%ZnO: Eu ³⁺ , Dy ³⁺	7.85	0.73	0.59	3.42
TiO ₂ /G/1.75%ZnO: Eu ³⁺ , Dy ³⁺	8.92	0.72	0.69	4.48
TiO ₂ /G/2.0%ZnO: Eu ³⁺ , Dy ³⁺	7.06	0.73	0.70	3.61
TiO ₂ /G/2.25%ZnO: Eu ³⁺ , Dy ³⁺	6.60	0.73	0.60	2.89
TiO ₂ /G/2.5%ZnO: Eu ³⁺ , Dy ³⁺	4.78	0.69	0.62	2.05

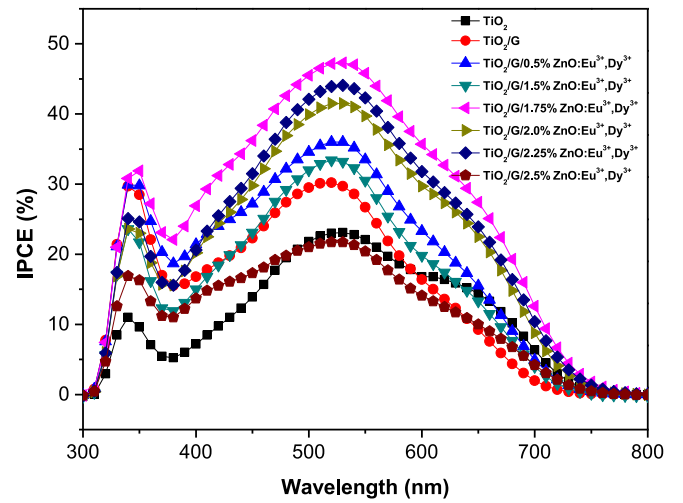


Fig. 7. IPCE spectra of the DSSCs based on pure TiO₂ structure, TiO₂/G structure and TiO₂/G/ZnO: Eu³⁺, Dy³⁺ structure.

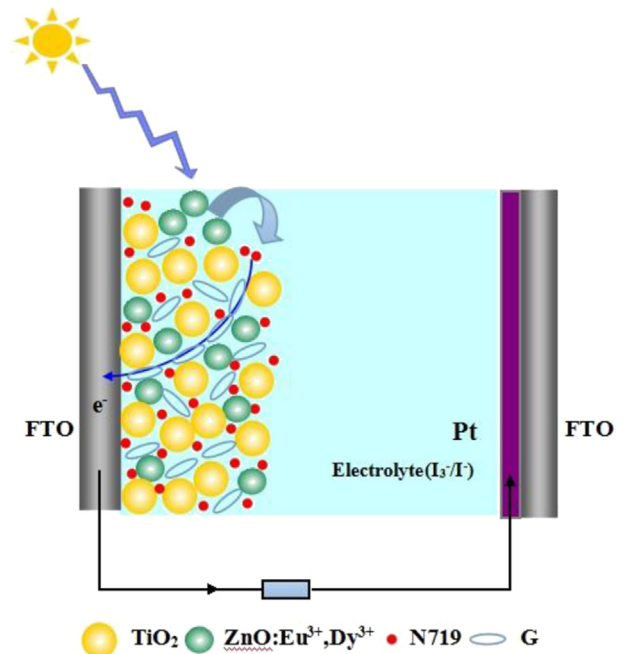


Fig. 8. The working process of DSSCs based on TiO₂/G/ZnO: Eu³⁺, Dy³⁺.

Acknowledgments

Project supported by the National Natural Science Foundation of China (Grant No. 61106059, 11304120), the Encouragement Foundation for Excellent Middle-aged and Young Scientist of Shandong Province (Grant No. BS2011NJ003, BS2012CL005, BS2013CL020), the Science-Technology Program of Higher Education Institutions of Shandong Province (Grant No. J11LA10).

References

- [1] B. O'Regan, M. Grätzel, *Nature* 353 (1991) 737–740.
- [2] C.Y. Chen, M. Wang, J.Y. Li, N. Pootrakulchote, L. Alibabaei, N.-L. Cevy-Ha, J.D. Decoppet, J.H. Tsai, C. Gratzel, C.G. Wu, S.M. Zakeeruddin, M. Grätzel, *ACS Nano* 3 (2009) 3103–3109.
- [3] B.E. Hardin, H.J. Snaith, M.D. McGehee, *Nat. Photonics* 6 (2012) 162–169.
- [4] M. Hamadani, A. Gravand, V. Jabbari, *Mat. Sci. Semicon. Proc.* 16 (2013) 1352–1359.
- [5] A. Yella, H.W. Lee, H.N. Tsao, C. Yi, A.K. Chandiran, M.K. Nazeeruddin, E.W. Diau, C.Y. Yeh, S.M. Zakeeruddin, M. Grätzel, *Science* 334 (2011) 629–634.
- [6] J. Zhang, H. Shen, W. Guo, S. Wang, C. Zhu, F. Xue, J. Hou, H. Su, Z. Yuan, *J. Power Sources* 226 (2013) 47–53.
- [7] H. Chang, C.H. Chen, M.J. Kao, S.H. Chien, C.Y. Chou, *Appl. Surf. Sci.* 275 (2013) 252–257.
- [8] Y.J. Chang, E.H. Kong, Y.C. Park, H.M. Jang, *J. Mater. Chem. A* 1 (2013) 9707–9713.
- [9] D. Li, P.C. Chang, C.J. Chien, J.G. Lu, *Chem. Mater.* 22 (2010) 5707–5711.
- [10] Q. Wang, T. Butburee, X. Wu, H. Chen, G. Liu, L. Wang, *J. Mater. Chem. A* 1 (2013) 13524–13531.
- [11] M. Kong, W. Hu, F. Cheng, Z. Huang, J. Zhang, Z. Han, N. Shi, Q. Fan, S. Chen, W. Huang, *J. Mater. Chem. C* 1 (2013) 5872–5878.
- [12] L. Li, Y.L. Yang, M. Zhou, R.Q. Fan, L.L. Qiu, X. Wang, L.Y. Zhang, X.S. Zhou, J.L. He, *J. Solid State Chem.* 198 (2013) 459–465.
- [13] G.B. Shan, G.P. Demopoulos, *Adv. Mater.* 22 (2010) 4373–4377.
- [14] W. He, T.S. Atabaev, H.K. Kim, Y.H. Hwang, *J. Phys. Chem. C* 117 (2013) 17894–17900.
- [15] Y.C. Chen, W.Y. Huang, T.M. Chen, *J. Rare Earth* 29 (2011) 907–910.
- [16] J. Liu, Q. Yao, Y. Li, *Appl. Phys. Lett.* 88 (2006) 173119.
- [17] U. Rambabu, S.D. Han, *Ceram. Int.* 39 (2013) 1603–1612.
- [18] T. Trupke, M.A. Green, P. Würfel, *J. Appl. Phys.* 92 (2002) 1668–1674.
- [19] Ü. Özgür, Y.I. Alivov, C. Liu, A. Teke, M.A. Reshchikov, S. Doğan, V. Avrutin, S.-J. Cho, H. Morkoç, *J. Appl. Phys.* 98 (2005) 041301.
- [20] K. Lü, G.X. Zhao, X.K. Wang, *Chin. Sci. Bull.* 57 (2012) 1223–1234.
- [21] Y. Wu, X. Zhang, J. Jie, C. Xie, X. Zhang, B. Sun, Y. Wang, P. Gao, *J. Phys. Chem. C* 117 (2013) 11968–11976.
- [22] J. Fan, S. Liu, J. Yu, *J. Mater. Chem.* 22 (2012) 17027–17036.
- [23] F.C. Krebs, *Sol. Energy Mater. Sol. Cells* 93 (2009) 394–412.
- [24] H. Yang, F. Peng, Q. Zhang, W. Liu, D. Sun, Y. Zhao, X. Wei, *Opt. Mater.* 35 (2013) 2338–2342.
- [25] T. Ling, J.G. Song, X.Y. Chen, J. Yang, S.Z. Qiao, X.W. Du, *J. Alloys Compd.* 546 (2013) 307–313.
- [26] E.M. Barea, J. Bisquert, *Langmuir* 29 (2013) 8773–8781.
- [27] Y. Wang, C. Feng, Z. Jin, J. Zhang, J. Yang, S. Zhang, *J. Mol. Catal. A Chem.* 260 (2006) 1–3.